

failure to detect such a configuration in the epr studies suggests that this result is not correct.

In the following paper,<sup>10</sup> the detailed mechanism by which the divacancy is formed in the damage event will be studied. There it is found that the threshold for production of these spectra is greater than that for the single vacancy. Also a preferential alignment of the defects with respect to the bombarding beam direction

is achieved. These serve as strong additional confirmation of the model.

#### ACKNOWLEDGMENTS

It is a pleasure to acknowledge the assistance of W. Colliton in all phases of the measurements. We are indebted to Dr. R. W. Redington for the use of the monochromator.

## Production of Divacancies and Vacancies by Electron Irradiation of Silicon

J. W. CORBETT AND G. D. WATKINS

General Electric Research Laboratory, Schenectady, New York

(Received 19 November 1964)

A study is described of the dependence of the room-temperature production of divacancies and vacancies in silicon upon the energy of the bombarding electrons over the range 0.7–56 MeV. For the divacancy, the Si-G6 electron-paramagnetic-resonance spectrum associated with the singly positively charged state of the defect was monitored. As a monitor for single-vacancy production, the Si-B1 center due to the oxygen-vacancy pair was used. Over the energy range 0.7–1.5 MeV, the divacancy production rate rises a factor of 7 while the single-vacancy rate rises only a factor of 1.5, reflecting a higher threshold for divacancy production, as expected. Also presented are data on the dependence of the divacancy production rate on the orientation of the crystal axes with respect to the incident beam and on the resulting anisotropy of the divacancy orientation in the lattice. The results of the anisotropy studies are shown to be consistent with a simple microscopic model of the damage event.

### I. INTRODUCTION

IN this paper, we present measurements of the dependence of the *direct* production of divacancies in silicon at room temperature upon the energy of the incident electrons. We also present data on the dependence of this production rate on the orientation of the crystal axes with respect to the incident beam, and on the resulting anisotropy of the divacancy orientation in the crystal lattice.<sup>1</sup>

For this study, the epr spectrum associated with the singly positively charged state of the divacancy (Si-G6)<sup>2</sup> was monitored. In order to assure that only divacancies produced as a primary damage event were observed, the study was performed in oxygen-doped (pulled) silicon. The oxygen is a good trap for mobile single vacancies,<sup>3,4</sup> inhibiting their agglomeration to form additional divacancies.

Also reported are measurements of the energy dependence of the room-temperature production of the oxygen-vacancy pairs. For this, the associated Si-B1<sup>5</sup>

epr spectrum was monitored. Since oxygen is a dominant trap for mobile vacancies in pulled silicon, the oxygen-vacancy pairs should serve as a reliable monitor of the *single-vacancy* production at room temperature.

It is found that the energy dependence for divacancies and oxygen-vacancy pairs are significantly different, reflecting a higher threshold energy for divacancy formation, as expected. In addition, the studies of the anisotropy of the divacancy production give insight into the details of the damage process.

### II. EXPERIMENTAL

The Si-G6 spectrum, used as the divacancy monitor, is observed when the Fermi level is below  $(E_v + 0.25)$  eV<sup>2</sup>; as a result, these measurements were performed on *p*-type (boron  $\sim 2 \times 10^{16}/\text{cm}^3$ ) pulled silicon.<sup>6</sup> The Si-B1 spectrum, used as the oxygen-vacancy pair monitor, is observed when the Fermi level is above  $(E_c + 0.17)$  eV<sup>3</sup>; for these studies, *n* type (phosphorus  $\sim 2 \times 10^{15}$  and  $5 \times 10^{16}/\text{cm}^3$ ) pulled silicon<sup>7</sup> was used. For all samples, production-rate studies were performed at low enough irradiation doses such that the Fermi level stayed locked to the original values. Under these conditions a linear production rate of spectra was observed versus integrated irradiation flux. This is a necessary feature of production-rate measurements and was always checked by at least two successive

<sup>1</sup> A preliminary report of this work was given in J. W. Corbett and G. D. Watkins, Phys. Rev. Letters **7**, 314 (1961).

<sup>2</sup> G. D. Watkins and J. W. Corbett, preceding paper, Phys. Rev. **138**, A543 (1965).

<sup>3</sup> G. D. Watkins and J. W. Corbett, Phys. Rev. **121**, 1001 (1961).

<sup>4</sup> J. W. Corbett, G. D. Watkins, R. M. Chrenko, and R. S. McDonald, Phys. Rev. **121**, 1015 (1961).

<sup>5</sup> This center was originally labeled the Si-A center and is discussed in Refs. 3 and 4. The new labeling scheme has been outlined in G. D. Watkins, *Proceedings of the Symposium on Radiation Damage in Semiconductors, Paris, 1964* (Dunod Cie, Paris, 1965, to be published).

<sup>6</sup> Purchased from DuPont Company.

<sup>7</sup> Kindly supplied by Dr. R. O. Carlson.

measurements to assure that they were in the linear region.

Each sample was 0.010 in.  $\times$  0.100 in.  $\times$  0.625 in. in size with a  $\langle 110 \rangle$  axis along the long dimension. For epr study a sample was sandwiched between two 0.045-in.  $\times$  0.100-in.  $\times$  0.625-in. silicon slabs and placed with the long dimension coaxial with the  $TE_{011}$  microwave cavity. The resulting square cross section of the "sandwich" was found to give a reproducibly good cavity  $Q$  as the samples were taken out, remounted, replaced, etc. In the divacancy measurements, the holder was made of 4- $\Omega$ -cm phosphorus-doped silicon ( $1.2 \times 10^{15}$  P/cm<sup>3</sup>) and the phosphorus epr spectrum in the (unirradiated) holder was exploited as a spectrometer sensitivity calibration for each run. In the measurements on the vacancy-oxygen pair, the holder was made of intrinsic silicon which gave no resonance signal. For these measurements, a small piece of 0.014  $\Omega$ -cm  $n$ -type silicon (As  $\sim 3 \times 10^{18}$ /cm<sup>3</sup>) was imbedded in one of the slabs of the holder and the conduction-electron resonance signal in this material was used as a calibrator.<sup>8</sup>

The spectra were measured with a balanced bolometer spectrometer at 20 kMc/sec, with 94-cps magnetic-field modulation and conventional lock-in techniques. For convenience, all measurements were made at 20.4°K, in dispersion. At this temperature, the widely different relaxation times for the various spectra gave different modes of spectrometer response for each.<sup>9</sup> For the phosphorus and conduction-electron resonance signals, the relaxation times were short, and normal, slow-passage derivatives of dispersion signals were recorded. For the Si-G6 and Si-B1 spectra,  $T_2$  and  $T_1$  were long enough to satisfy the adiabatic-fast-passage condition during the modulation cycle. For the Si-G6 spectrum,  $\omega_m T_1 \ll 1$ , giving an absorption-like signal 90° out of phase with the modulation (at frequency  $\omega_m$ ). For the Si-B1 spectrum,  $\omega_m T_1 \gg 1$ , and an absorption-like signal in phase with the modulation was observed. For relative measurements on a single spectrum (versus energy, dose, beam-direction, etc.) these differences were not important and it was sufficient to monitor only an amplitude of a specific spectral component as a measure of the concentration.

However, in order to relate the measured amplitude of each spectrum at 20.4°K to the *absolute* concentration of the corresponding defect, the following additional calibration experiment was performed. By lowering the temperature, both the Si-G6 and the phosphorus (in the holder) resonances could be brought into the same operating mode as that for Si-B1 at 20.4°K ( $\omega_m T_1 \gg 1$ ). In this mode, the area of each spectrum was

<sup>8</sup> In these measurements, the phosphorus signal in the irradiated material was also monitored; hence this different calibration signal was required.

<sup>9</sup> For a discussion of these effects see A. M. Portis, Phys. Rev. **100**, 1219 (1955), and Technical Note No. 1, Sarah Mellon Scientific Radiation Laboratory, University of Pittsburgh, 1955 (unpublished); M. Weger, Bell System. Tech. J. **39**, 1013 (1960).

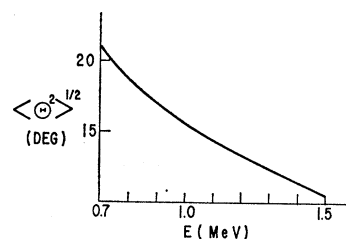


Fig. 1. Calculated rms multiple scattering angle versus electron energy after penetration of the beam halfway through the 0.010-in.-thick silicon sample.

measured on the recording and corrected to the equivalent area at 20.4°K by the difference in the Boltzmann factor. These corrected areas were then taken to be proportional to the concentration of defects. With the known phosphorus concentration in the reference sample, a conversion factor was thus obtained for each spectrum relating the absolute concentration of defects to the amplitudes measured at 20.4°K. We estimate the accuracy of this calibration to be within a factor of 2 for each spectrum. The reproducibility and general consistency of the results appear to be within this estimate. We do not attempt to refine it beyond this because there remain uncertainties that are difficult to evaluate (such as the possible lack of exact equivalence between the response of the different spectra, etc.). The accuracy of *relative* measurements on a single spectrum should be more accurate.

Most of the irradiations were performed at  $\leq 1.5$  MeV with electrons from a G.E. resonant transformer accelerator, gated so that current flowed only during a 36° sector of the voltage peak. The total spread in energy of the electrons was  $\sim 10\%$  of the maximum energy.<sup>10</sup> The samples were placed with the thin side perpendicular to the beam direction. Irradiations along the  $\langle 100 \rangle$ ,  $\langle 110 \rangle$ , and  $\langle 111 \rangle$ <sup>11</sup> crystallographic directions were carried out. The irradiation flux was calibrated using an evacuated Faraday cage. The beam was homogeneous to  $\pm 10\%$  over the surface of the samples. The current was  $\leq 3 \mu\text{A}/\text{cm}^2$  and the samples were cooled by an air blast. It is estimated that the sample temperature did not exceed 70°C during the irradiation.

The choice of sample thickness (0.010 in.) represented a compromise between the increased epr signal-to-noise ratio for thick samples on the one hand and, on the other, the improved energy and beam-direction resolution as the sample is made thinner. We may make a rough estimate of the energy resolution as follows: The average energy loss<sup>12,13</sup> in penetrating the 0.010-in.

<sup>10</sup> The detailed energy distribution in our accelerator has been discussed previously—see J. W. Corbett, J. M. Denney, M. D. Fiske, and R. M. Walker, Phys. Rev. **108**, 954 (1957), in particular, Fig. 6.

<sup>11</sup> For convenience, some of the  $\langle 111 \rangle$  irradiations were performed by tipping a  $\langle 110 \rangle$  sample 35° so that its  $\langle 111 \rangle$  axis was along the beam direction. A simultaneous irradiation of both a  $\langle 111 \rangle$  oriented slab and a tipped  $\langle 110 \rangle$  one checked the equivalence of the two within the accuracy of measurement.

<sup>12</sup> See W. Heitler, *Quantum Theory of Radiation*, (Oxford University Press, London, 1954), Sec. 37.

<sup>13</sup> Since the average loss is greater than the most probable loss, such an estimate is conservative, taking into account in a rough way the additional spreading due to straggling as well.

sample varies from 105 to 100 keV for beam energies from 0.7 to 1.5 MeV. Averaged over the sample, this is equivalent to an infinitesimally thin sample irradiated by electrons with a roughly flat distribution over this energy range. Combining this with the  $\sim 10\%$  spread in energy from the accelerator, we estimate an effective resolution in our measurements which varies from  $\sim 130$  to 180 keV over the range 0.7 to 1.5 MeV.

Shown in Fig. 1 is the calculated<sup>14</sup> rms multiple scattering angle corresponding to penetration of the beam halfway through the 0.010-in. sample. This angle is a measure of the spread in the high-energy electron direction and defines an effective angular resolution for the angular dependence studies.

In plotting the experimental results versus beam energy, the average energy corresponding to the penetration of the beam halfway through the sample was used. This includes a correction ( $\sim 36$  keV) for the energy loss in the accelerator exit window and intervening air, as well as an average over the current sector of the accelerator.

The irradiations at 13 and 56 MeV were performed on the Rensselaer Polytechnic Institute linear accelerator by Professor J. C. Corelli. The flux measurements for these preliminary irradiations were less accurate, the current being monitored simply by collection in an unshielded aluminum cup. The calculated production rates at these energies are therefore correspondingly less accurate. It is difficult to estimate the accuracy and we therefore present the results at these energies only as rough guides to the production rates.

### III. RESULTS AND DISCUSSION

#### A. Production-Rate Studies

Figure 2 summarizes the results of the production-rate studies of the divacancy in the energy region 0.7–1.5 MeV. The indicated value for the production rate includes all divacancies formed, regardless of orientation in the lattice, as monitored by the total intensity

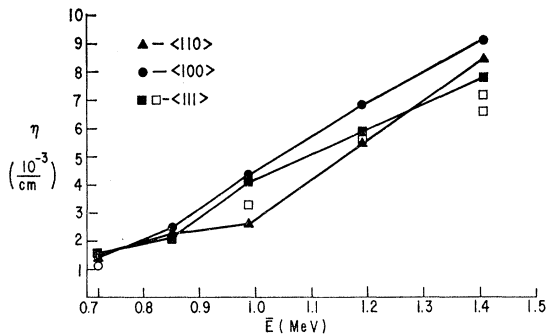


FIG. 2. Divacancy production rates versus electron energy and incident-beam direction (see legend).

<sup>14</sup> G. Molière, *Z. Naturforsch.* **2a**, 133 (1947), **3a**, 78 (1948); A. O. Hanson, L. H. Lanze, E. M. Lyman, and M. B. Scott, *Phys. Rev.* **84**, 634 (1951).

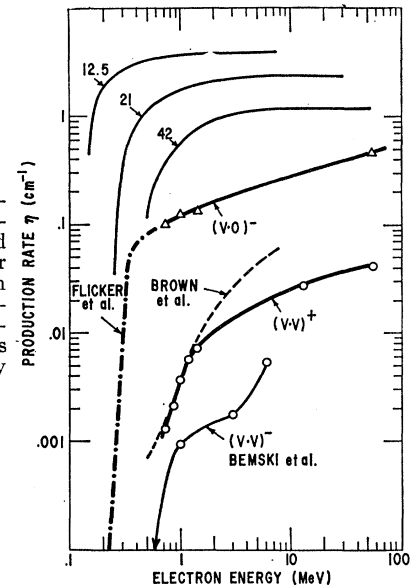


FIG. 3. Energy dependence of divacancy  $(V \cdot V)^+$  and oxygen-vacancy pair  $(V \cdot O)^-$  production rates, with comparison to other experimental measurements and simple theory (see text).

of the Si-G6 spectrum. The dependence of this rate on the direction of the incident beam with respect to the crystal axes is also indicated. The closed points denote experiments in which the irradiations for all three orientations were performed simultaneously. Such measurements should be relatively accurate in showing the relationship between the orientations. The open squares show independent  $\langle 111 \rangle$  irradiations and reflect the over-all reproducibility of the measurements.

We note that the  $\langle 100 \rangle$  production rate is uniformly the highest. This is different from what has been inferred from electrical studies of damage in silicon<sup>15</sup> and germanium.<sup>16</sup> There, carrier removal experiments indicate an ordering of damage production rates of  $\langle 111 \rangle > \langle 110 \rangle > \langle 100 \rangle$ . Presumably, the difference is that here we are looking only at divacancies, while the carrier removal studies reflect the production of other defects as well, and may be dominated by the more abundant defects arising from single-vacancy production.

We note also that there is a large (factor  $\sim 7$ ) increase in the production rate over this narrow energy range. In Fig. 3 we plot the  $\langle 111 \rangle$  results on a log-log plot and include the provisional determinations at 13 and 56 MeV. Above 1.5 MeV, the production rate is observed to rise more slowly.

We also show in Fig. 3 data taken by Bemski, Szymanski, and Wright.<sup>17</sup> They made measurements on the energy dependence of the production rate of the Si-G7 spectrum in *n*-type silicon. The arrow on their data in Fig. 3 indicates they found no Si-G7 defects

<sup>15</sup> V. S. Vavilov, V. M. Patskevich, B. Ya Yurkov, and P. Ya. Glazunov, *Fiz. Tverd. Tela* **2**, 1431 (1960) [English transl.: *Soviet Phys—Solid State* **2**, 1301 (1961)].

<sup>16</sup> W. L. Brown and W. M. Augustyniak, *J. Appl. Phys.* **30**, 1300 (1959).

<sup>17</sup> G. Bemski, B. Szymanski, and K. Wright, *J. Phys. Chem. Solids* **24**, 1 (1963).

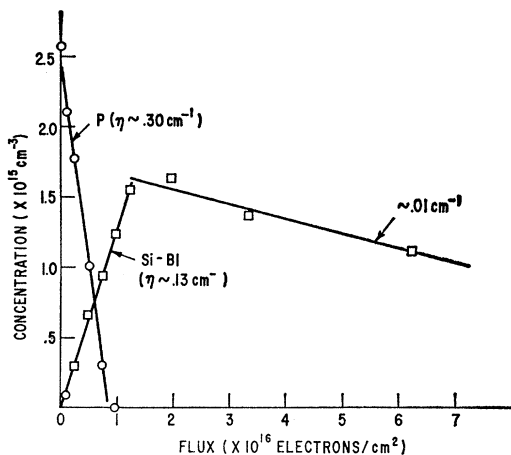


FIG. 4. Intensity of the spin-resonance spectra in pulled  $n$ -type silicon versus electron dose. The average electron energy was 1.41 MeV.

produced for bombardment at 500 keV. Because of this large energy dependence, they speculated that the Si-G7 spectrum was due to a higher order defect, specifically suggesting the divacancy. In the preceding paper<sup>2</sup> we showed conclusively that the Si-G7 spectrum is indeed due to the divacancy. We further showed, however, that this resonance is not normally observed for the Fermi level close to the conduction band as was apparently the condition of their experiment,<sup>18</sup> but rather that it is necessary for the Fermi level to be near the center of the forbidden gap. This could account for the discrepancy between the Bemski *et al.* data and ours—their data not measuring all the defects present but rather only a small fraction in the suitable non-equilibrium charge state perhaps resulting from stray light shining on the sample.<sup>19</sup>

In Fig. 3 we also present the results for the oxygen-vacancy pair. The production rate is an order of magnitude greater than the divacancy rate and rises only gradually versus energy over the whole energy range. In particular, there is a large difference in the energy dependence for the two in the 0.7–1.5-MeV range (a factor of 1.5 increase for the oxygen-vacancy pair versus a factor of 7 for the divacancy). This clearly demonstrates a higher threshold energy for the divacancy formation.

[*Note added in proof.* Subsequent experiments in which the samples for the  $(V \cdot O)^-$  and the  $(V \cdot V)^+$  measurements were irradiated simultaneously, show that the ratio of the production rates  $[(V \cdot O)^- / (V \cdot V)^+]$  is 5.4 at 14 MeV and 3.3 at 52 MeV. The two production rate curves are therefore converging at high energies

<sup>18</sup> In Fig. 2 of Ref. 17, we note the strong resonance of the phosphorus donor. This suggests that the Fermi level was still at  $(E_c - 0.05)$  eV, the position of the donor.

<sup>19</sup> We do not mean to exclude the possibility that the divacancy production rate may differ in  $n$ - and  $p$ -type silicon. However, we believe the difference is not so great as to account for the discrepancy between the data of Bemski *et al.* and ours. See footnote 27.

somewhat more rapidly than the preliminary high-energy data in Fig. 3 indicated.]

Flicker, Loferski, and Scott-Monck<sup>20</sup> have recently measured the energy dependence of damage in silicon in the range 125–800 keV. They used the deterioration of minority carrier lifetime as observed in a  $p$ - $n$  junction as monitor. We show their data in Fig. 3 (by the dash-dot line) arbitrarily adjusted to fit our data for the oxygen-vacancy pair at 700 keV. (Their measurements only indicate relative energy dependence so a comparison on an absolute basis is not possible.) The rationale for matching their data to the oxygen-vacancy pair data is that they observed only a small energy dependence between 400 and 800 keV. In view of the large divacancy dependence observed by us we conclude that the damage observed by them is a result of single vacancy production, as is the vacancy-oxygen pair.

Above 800 keV, however, minority carrier lifetime damage in solar cells has been reported to rise abruptly.<sup>21,22</sup> This has led to the suggestion<sup>21,22</sup> that divacancy and higher multiple defect formation may be the cause. We show in Fig. 3 the degradation rate of  $n$ -on- $p$  solar cells versus energy as given by Brown, Gabbe, and Rosenzweig<sup>22</sup> arbitrarily normalized to our divacancy production curve at 1 MeV. The close similarity of the curves in the 0.7–1.5-MeV region gives support to this interpretation. The apparent departure at higher energies could be the result of higher order defect production (trivacancies, etc.), although the uncertainty in our higher energy flux calibration could be the source of the discrepancy.

Finally, in Fig. 3, we also show the theoretical prediction for a simple step-function displacement probability function with thresholds of 12.5, 21, and 42 eV, for single-vacancy production.<sup>23</sup> These calculations do not include multiple atom-displacement effects.<sup>24</sup> As is well known from electrical studies in silicon and germanium, measurements such as ours which are still well above threshold tend to indicate threshold energies that are too large. For instance, ignoring the large discrepancy in absolute magnitude, the Flicker *et al.* data as presented here might suggest a threshold  $\sim 21$  eV. However, their results followed to lower energies indicate a much lower threshold of  $\sim 12$ –13 eV, as previously determined by Loferski and Rappaport.<sup>25</sup>

<sup>20</sup> H. Flicker, J. J. Loferski, and J. Scott-Monck, *Phys. Rev.* **128**, 2557 (1962).

<sup>21</sup> J. J. Wysocki, *J. Appl. Phys.* **34**, 2915 (1963).

<sup>22</sup> W. L. Brown, J. D. Gabbe, and W. Rosenzweig, *Bell System Tech. J.* **42**, 1505 (1963).

<sup>23</sup> Here the form of the electron-nucleus cross section given by W. A. McKinley, Jr. and H. Feshbach [*Phys. Rev.* **74**, 1759 (1948)] was used.

<sup>24</sup> This omission seems appropriate here since multiple displacements imply vacancies in close proximity with one another. These could in turn recombine to form divacancies and higher aggregates, which would not show up as simple vacancy-oxygen pairs.

<sup>25</sup> J. J. Loferski and P. Rappaport, *Phys. Rev.* **111**, 432 (1958); *J. Appl. Phys.* **30**, 1296 (1959).

It is still a convenient concept, however, to refer to an effective threshold (of 21 eV in this case) in this energy range. With this in mind, it is instructive to note the similarity of the divacancy curve to the shape of the 42-eV threshold curve. A simple model of divacancy formation predicts a threshold just twice that for single-vacancy production.

In Fig. 4 we show a typical set of data from which the oxygen-vacancy-pair production rate was determined. For this run, the average bombarding energy was 1.41 MeV and, as for all the other oxygen-vacancy pair studies, the bombarding direction was a  $\langle 100 \rangle$  axis. As the amplitude of the Si-B1 spectrum grows, we note also the decrease of the resonance of the electrons at the phosphorus donor sites. This decrease occurs because the electrons are being removed to populate the deeper levels produced by the irradiation [e.g., the vacancy-oxygen pair at  $(E_c - 0.17)$  eV]. The decrease in the phosphorus resonance is therefore related to the cross-carrier removal rate, measured in electrical studies.<sup>26</sup>

As is also shown in Fig. 4, the amplitude of the Si-B1 spectrum eventually reaches a maximum and then slowly decreases with increasing flux. The decrease results from the removal of electrons from the  $(E_c - 0.17)$  eV level by levels being produced still deeper in the gap. As was shown in the preceding paper<sup>2</sup> the divacancy introduces a double acceptor level at  $\sim (E_c - 0.4)$  eV. The measured divacancy production rate in *p*-type silicon at this energy (Fig. 2) is  $\sim 0.008$  cm<sup>-1</sup>. Assuming the divacancy production rate to be the same in *n*-type material, and with two electrons removed per defect, this would cause a removal rate of  $\sim 0.016$  cm<sup>-1</sup>. The rough agreement with the observed value of 0.010 cm<sup>-1</sup> in Fig. 4 suggests that in this experiment the divacancy is the dominant deeper level.<sup>27</sup> This is not always so. In pulled samples doped with  $\sim 5 \times 10^{16}$ /cm<sup>3</sup> phosphorus, we have observed a non-linear production rate of the Si-B1 centers and a faster decrease of the Si-B1 amplitude, both of which could be interpreted as due to the competition of the phosphorus with the oxygen as trapping centers for the

<sup>26</sup> The apparent discrepancy between the phosphorus removal rate and the Si-B1 center production rate is almost within the factor-of-2 error for the absolute values and therefore may not be real. However, the data could be interpreted as indicating that another defect is being produced which has an acceptor level between the phosphorus and Si-B1 center levels. The continued increase in the Si-B1 spectrum observed after the phosphorus resonance has disappeared could result from the further removal of electrons from this intermediate level. Its production rate could be comparable to that for the Si-B1 center. No evidence of such a level has been reported in electrical measurements but of course if it were near either the phosphorus or the Si-B1 center levels it would be hard to distinguish it in the electrical measurements. Further experiments are necessary to explore this.

<sup>27</sup> Continued to higher doses, the Si-B1 center disappears and the Si-G7 spectrum associated with the singly negatively charged state of the divacancy eventually emerges. A rough estimate of the divacancy production rate from the amplitude of this spectrum is consistent with these other estimates.

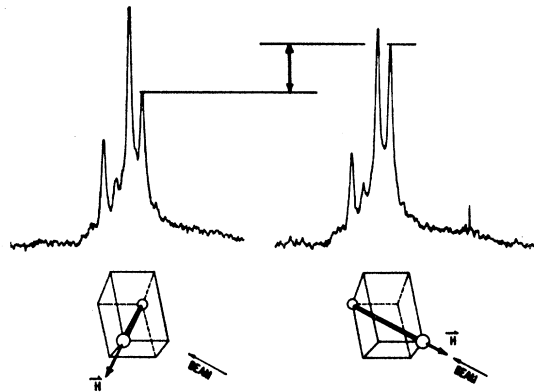


FIG. 5. Si-G6 divacancy spectrum with magnetic field  $H$ , (a) parallel to the incident  $\langle 111 \rangle$  beam direction and (b) parallel to a different  $\langle 111 \rangle$  axis. The average electron energy was 0.99 MeV. Magnetic field increases to the left for each recording.

vacancies. [The vacancy-phosphorus pair has a deeper level also at  $\sim (E_c - 0.4)$  eV.]<sup>28</sup>

### B. Anisotropy of Divacancy Production

In these experiments the beam direction was along a  $\langle 111 \rangle$  direction. After irradiation, the Si-G6 spectrum with the magnetic field along the beam direction was compared to that with the magnetic field along a different  $\langle 111 \rangle$  direction in the crystal. A typical result (average electron energy  $\bar{E} = 0.99$  MeV) is shown in Fig. 5. As has been shown in the preceding paper,<sup>2</sup> under these conditions the intensity of the low-field multiplet is directly proportional to the number of divacancies whose vacancy-vacancy axes lie along the magnetic field. From the figure we see that considerably more divacancies have their axes along the beam direction than along the other  $\langle 111 \rangle$  direction.

In Fig. 6, we show the anisotropy  $R$  versus energy, where  $R$  is the ratio of the number of divacancies along the  $\langle 111 \rangle$  beam axis to the number in each of the other

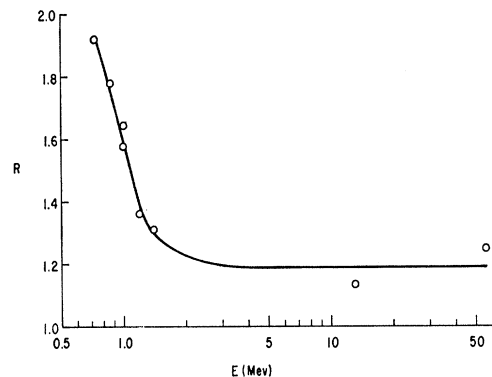


FIG. 6. Anisotropy  $R$  of the divacancy orientation versus bombarding electron energy.  $R$  is the ratio of the number of divacancies along the beam axis to that along another  $\langle 111 \rangle$  axis.

<sup>28</sup> G. D. Watkins and J. W. Corbett, Phys. Rev. **134**, A1359 (1964).

$\langle 111 \rangle$  axes. (They each make an angle of  $70^\circ 31'$  with respect to the beam direction.) It is seen that the ratio is strongly energy-dependent becoming larger at lower energies.<sup>30</sup> It is interesting to note, however, that a definite anisotropy persists even out to 56 MeV.

The anisotropy can be removed by annealing the sample above room temperature. It is found that the recovery follows kinetics identical to that for the stress-induced alignment described in the preceding paper<sup>2</sup> (see Fig. 11 of that reference), confirming that the two are entirely equivalent.

As mentioned before, the Si-G7 spectrum for the negatively charged divacancy is not as suitable for study because it is observed only in high-resistivity *n*-type material. However, in order to confirm that this center also has the same anisotropy, one *p*-type sample was irradiated long enough to convert it to high-resistivity *n* type for study. Within experimental accuracy, the same degree of preferential alignment was found in the resulting Si-G7 spectrum as was observed in the Si-G6 spectrum under the same conditions.

The anisotropy proves in a striking way that the divacancies were produced as a primary event. They have a built-in memory of the direction in which the primary bombarding electron was going. In addition, the sense of the anisotropy gives some insight into the actual production process. In the damage event, a high-energy electron collides with the nucleus of a single atom imparting recoil energy to it. In order to create a divacancy, this atom must in turn collide with a neighbor atom causing it to be displaced into the lattice as an interstitial. In addition, the initial recoil atom must retain enough energy so that it too becomes an interstitial. The highest energy recoil for the primary atom is along the beam direction. As the beam energy is reduced, a point is ultimately reached where sufficient energy is available to produce a divacancy along the beam direction but not in the other three  $\langle 111 \rangle$  directions,  $70^\circ 32'$  away.

We have, therefore, demonstrated that the threshold for divacancy damage production depends upon the orientation of the beam and the resulting divacancy direction. Referring to Fig. 2, it is interesting to speculate that the "break" seen in the  $\langle 110 \rangle$  curve at  $\sim 1$  MeV is due to the onset of divacancy production along the  $\langle 111 \rangle$  at  $90^\circ$  to the beam. We might expect the break to be most evident in these  $\langle 110 \rangle$  irradiations because the full  $90^\circ$  angle would give the highest

<sup>29</sup> The values of the anisotropy shown in Fig. 6 are due to improved measurements and are larger than those given in our preliminary report (see Ref. 1).

threshold. Unfortunately, the geometry of the samples was not favorable for study of the anisotropy directly to check this.

#### IV. SUMMARY

Because of the detailed information available in an epr spectrum both as regards the defect identification and its orientation in the lattice, we have been able to determine highly specific information about some of the damage production processes in silicon with high-energy electrons. It is our hope that this kind of information will interest theorists in silicon as a medium for calculations of the details of the damage process. Computer calculations of the damage process in copper<sup>30</sup> and iron,<sup>31</sup> for instance, have generated highly specific models for defects and processes in systems which are not experimentally conducive to the spectroscopic tools which could check the theory. Admittedly in these systems, the theorist is somewhat safer as regards the form of the interaction potential to use, etc. A covalent, tetrahedrally-coordinated semiconductor, is presumably much harder to handle. On the other hand, the detailed microscopic information available through epr studies is not an insignificant compensation.

Throughout this paper we have assumed that the Si-G6 spectrum has been proven to be associated with the divacancy and have used it then as a tool to study the details of the production process. Reversing the arguments for the moment, we should also point out that the results found here serve as strong additional confirmation of this identification. The important results in this regard are (i) the threshold energy for formation higher than that for single vacancies, (ii) the anisotropy of the defect alignment with respect to the beam direction and its simple interpretation in terms of the model. The observation of identical anisotropy for the Si-G7 spectrum is a strong additional confirmation of it as a different charge state of the same divacancy.

#### ACKNOWLEDGMENTS

The authors thank Professor J. C. Corelli of Rensselaer Polytechnic Institute for performing the 13- and 56-MeV irradiations at the R.P.I. Linac Laboratory. They also thank W. Colliton for materially assisting in all phases of the experimental work.

<sup>30</sup> J. B. Gibson, A. N. Goland, M. Milgram, and G. H. Vineyard, *Phys. Rev.* **120**, 1229 (1960); G. H. Vineyard, *Disc. Faraday Soc.* **31**, 7 (1961); G. H. Vineyard in *Radiation Damage in Solids* edited by D. S. Billington (Academic Press, Inc., New York, 1962), p. 291.

<sup>31</sup> G. Erginsoy, G. H. Vineyard, and A. Englert, *Phys. Rev.* **133**, A595 (1964); J. R. Beeler, Jr. and D. G. Besco, *Bull. Am. Phys. Soc.* **9**, 284 (1964).